CRYSTAL GROWTH & DESIGN
2003
VOL. 3, NO. 3
301−311

The Aryl Bromine−Halide Ion Synthon and Its Role in the Control of the Crystal Structures of Tetrahalocuprate(II) Ions

Roger D. Willett,* Firas Awwadi, and Robert Butcher

Department of Chemistry, Washington State University, Pullman, Washington 99164

Salim Haddad

Department of Chemistry, University of Jordan, Amman 11942, Jordan

Brendan Twamley

University Research Office, University of Idaho, Moscow, Idaho 83844

Received January 14, 2003

ABSTRACT: The role of the arylbromine-halide ion (C−Br···X$^-$) synthons in the development of the supramolecular frameworks is explored in a set of six bromopyridinium tetrahalocuprate(II) salts. The compounds belong to the series $(n\text{BP})_2\text{CuX}_4$, where $n\text{BP}^+$ denotes the *n*-bromopyridinium cation and $n = 2$, 3, or 4 and X = Cl$^-$ or Br$^-$ and include $(2\text{BP})_2\text{CuBr}_4$, $(3\text{BP})_2\text{CuBr}_4$, $(4\text{BP})_2\text{CuBr}_4$, $(2\text{BP})_2\text{CuCl}_4$, $(3\text{BP})_2\text{CuCl}_4$, and $(4\text{BP})_2\text{CuCl}_4$. The structures all consist of isolated pyridinium cations and flattened tetrahedral CuX_4^{2-} anions. The supramolecular assembly of these ionic species is dominated by the novel C−Br···X$^-$ synthon and the more traditional N−H···X$^-$ synthon. The C−Br···X$^-$ synthon is invariably characterized by essentially linear C−Br···X$^-$ angles with Br···X$^-$ contacts 0.3−0.4 Å less than the sum of the van der Waals radii. In contrast, the N−H···X$^-$ synthons show a variety of geometries: linear, symmetric bifurcated, and asymmetric bifurcated. In all cases, low dimensional supramolecular networks are developed based on combinations of the C−Br···X$^-$ and N−H···X$^-$ synthons. These include chain networks in $(3\text{BP})_2\text{CuCl}_4$, $(4\text{BP})_2\text{CuBr}_4$, and the $(4\text{BP})_2\text{CuX}_4$ salts. A double chain network exists in $(3\text{BP})_2\text{CuBr}_4$, while the structure of $(4\text{BP})_2\text{CuCl}_4$ contains a two-dimensional network. A common feature in all six networks is the existence of bibridged $[\text{CuX}_4^{2-} - (n\text{BP}^+)_2 - \text{CuX}_4^{2-}]$ units, while the more complex double chain and layer networks also contain monobridged $[\text{CuX}_4^{2-} - (n\text{BP}^+) - \text{CuX}_4^{2-}]$ units. These units then aggregate into the final crystal structures generally with coplanar stacking of the substituted pyridinium cations. The stacking interactions between cations include both $\pi-\pi$ and π−Br interactions. In general, the $\pi-\pi$ stacking is not optimal and, in some cases, it is nonexistent. Comparison with other previous studies show the competitive nature of the C−Br···X$^-$ and N−H···X$^-$ synthons in halocuprate(II) structures.

Introduction

The identification of weak noncovalent interactions between chemical species in crystalline materials and the understanding of the role that these interactions play in the determination of supramolecular structure is one of the major foci in crystal engineering today.[1] Some of these, such as the hydrogen bonding and $\pi-\pi$ stacking interactions, have long been recognized as playing a crucial role in the development of supramolecular structures. The greatest successes in the area of crystal engineering occur with molecules that contain a limited number of complementary groups that define supramolecular synthons that have well-defined directional properties. The most widely studied of these synthons is the hydrogen bonding interaction between oxygen and/or nitrogen donors and acceptors. This interaction is quite strong and often has predictable directional properties. Thus, numerous examples of useful materials have been synthesized by careful design of the organic entities containing the groups involved in the hydrogen bonds. (See Aakeröy and Beatty for a recent review.[2]) These include guest−host systems, catalysts, and nonlinear optical materials to name a few. However, in these studies, it is clear that other, weaker interactions can play a significant role in the determination of the final structures. Such competitive interactions provide diversity in the observed structures as well as uncertainty in the structure predictions. Thus, for example, Garden et al.[3] have examined the competitive effects of hydrogen bonding, iodo-nitro interactions, and aromatic $\pi-\pi$ stacking in iodo-nitroanilines. One of the challenges of crystal engineering today is the clarification of the relative roles of the various synthons in supramolecular structures.

The role of organohalides in the development of supramolecular structure has been receiving increasing attention. Systems containing the C−X···N−C synthon have been the subject of one set of such studies. Here organohalides such as tetraiodotheylene or tetraiodidemethane have been shown to form donor−acceptor complexes with both aromatic and aliphatic polyamines.[4] Pennington et al. have emphasized the advantage of organiodides over molecular iodine in crystal engineering studies.[4b,c] Another group of studies has focused on C−X···X−C interactions and have included both experimental and theoretical studies.[5] Two types of such interactions have been observed based on the values of the C−X···X and X···X−C angles: (a) type I, the symmetrical arrangement (both angles equal, but rarely 180°) and (b) type II, the 180°−90° perpendicular

10.1021/cg030003y CCC: $25.00
Published on Web 04/19/2003

arrangement. Several authors have studied structures with triangular arrays of halogen atoms that involve the 180−90° C−X···X−C arrangement. The geometrical features of these interactions have been rationalized by a nonspherical electrostatic potential about the halogen atom, with a positive potential in the σ region and a negative potential in the π region of the atom.[6] A study by Csöregh et al. has focused on the competitive interactions between C−X···X−C and O−H···O synthons in a series of halogen substituted diols.[7] In addition, Bishop and co-workers, as well as others, have also identified a stacking pattern involving π−halogen interactions in arylhalide compounds.[8] In this pattern, the arylhalide moieties stack in an antiparallel fashion to form dimeric structures.

Another type of organohalide synthonic interaction is that with halide ions. Given the charge distribution around the C−X moiety, a linear C−X···X^- interaction is to be expected, and is supported by the reported studies. A number examples and applications of C−X···X^- interactions have appeared in the literature, beginning with the extensive study of the complexes of tetraalkyammonium salts with simple alkyl halides in 1972 by Creighton and Thomas.[9a] Farina, et al. cite the example of the resolution of a racemic perfluoralkylbromide that was made enantiomorphically pure by crystallization with a chiral alkylammonium bromide, the crystallization being facilitated by the C−Br···Br^- interactions.[9b] Freytag, et al. have taken advantage of these interactions in the design of a series of (4-halopyridinium) halide salts (halo, halide = Cl, Br, I).[9c] The structures consist of linear arrays of cations and halide ions held together by N−H···X^- and C−X···X^- interactions. In all three, the C−X···X^- supramolecular interactions are nearly linear (the C−X···X^- angles are all greater than 160°). More complex systems involving C−X···X and C−X···X^- interactions arise in a series of halogen and polyhalide ion salts of halogenated tetrathiafulvalenes,[10a] while Yamamoto et al. have prepared molecular conductors in which halide ion salts of EDT-TTF type donor−acceptor complexes are cocrystallized with organohalides such diiodoacetylene.[10b] Here the halogen−halogen or halogen−halide interactions appear to contribute to the conductive properties in these systems. Other authors have noted the presence of short C−X···X^- contacts in a variety of compounds and have discussed them in varying detail.[11] These studies would indicate that the linear C−X···D synthon (D = donor) can be a strong contributor to the formation of the supramolecular structure in a variety of situations

Interest in the structure of hybrid organoammonium halocuprates has arisen because of novel magnetic systems that have been found in a number of A_2CuBr_4 salts that contain distorted tetrahedral anions.[12] In these salts, it has been realized that significant antiferromagnetic exchange coupling may occur through so-called two-halide (2H) exchange pathways. These pathways can involve relatively long contacts (up to 0.5 Å longer than the sum of the van der Waals radii) between halide ions on neighboring copper(II) centers. The systems studied to date include two-dimensional S = $^1/_2$ antiferromagnetic systems and a variety of ladder systems with varying rations of J_{rung}/J_{rail}.[13] These studies provide important information concerning the physics of these systems.

The crystal engineering challenge with these systems is to find rational synthetic schemes to generate the desired 2H contact pathways. With other copper(II) halide systems, we have had considerable success in the design and/or rationalization of several structural types based on dimensional reduction arguments.[14] In this process, crystallization in the presence of appropriate organoammonium halides has been used to break a higher dimensional structure into lower dimensional fragments. The design and characterization of layered perovskites of the type $(RNH_3)_2MX_4$ or $(NH_3RNH_3)MX_4$ derived from the parent AMX_3 perovskite structure is the premier example of the success of crystal engineering in this area.[15] Unfortunately, for the A_2CuBr_4 systems based on isolated $CuBr_4^{2-}$ anions, no such dimensional reduction scheme is readily applicable. Thus, synthesis of these materials has been very much a hit or miss process.

To meet this challenge, the role of N−H···X^- and π−π interactions in the development of the supramolecular structure of hybrid organic/inorganic metal halide salts has recently begun to receive specific attention. Freytag et al. have utilized 4,4′-bipyridinium cations to develop linear chain structures with $(MX_n)^{2-n}$ anions.[12] With this symmetrical dication, bifurcated N−H···X^- interactions play dominant roles in a variety of tetrahalometalate salts, thus giving directional control of the hydrogen bonding interactions. Luque et al. have examined the series of compounds $(pyH)_2CuBr_4$, $(n\text{-}MepyH)_2CuBr_4$, and $(n\text{-}EtpyH)_2CuBr_4$ (n = 2, 3, 4) where linear chain structures are again observed.[13] However, in these cases, the N−H···X^- hydrogen bonds form $(s\text{-}pyH)_2CuBr_4$ molecular units (s-py = substituted pyridine), and the chain structure is propagated by π−π stacking between s-pyH^+ cations on adjacent molecular units. We have recently shown these interactions to be important factors in the structures of a variety of $(4DMAP)_2MX_3$ and $(4DMAP)_2MX_4$ salts, where 4DMAP is the 4-dimethylaminopyridinium cation.[14]

In the process of studying these types of systems, we and others have frequently observed halogenation of the organic cations employed, particularly when the halogen involved is bromine. Reexamination of these structures has shown the presence of short, linear C−X···X^- interactions in many of them. Consequently, we have begun a systematic study of the crystal structures of the copper(II) halide complexes with mono- and dibromosubstituted pyridine and pyridinium halides. The goal is to understand the competitive interplay of the N−H···X^- and C−X···X^- synthons, and to see if this can be utilized to better control the supramolecular structures in these systems.

In this paper, we examine the structures of a series of six copper(II) halide salts with *n*-bromopyridinium cations (n = 2, 3, and 4): (1) $(2BP)_2CuBr_4$, henceforth 2BP−Br; (2) $(3BP)_2CuBr_4$, henceforth 3BP−Br; (3) $(4BP)_2CuBr_4$, henceforth 4BP−Br; (4) $(2BP)_2CuCl_4$, henceforth 2BP−Cl; (5) $(3BP)_2CuCl_4$, henceforth 3BP−Cl; and (6) $(4BP)_2CuCl_4$, henceforth 4BP−Cl. These structures will clearly show that the aryl-C−Br···X^- interaction is a very significant supra-

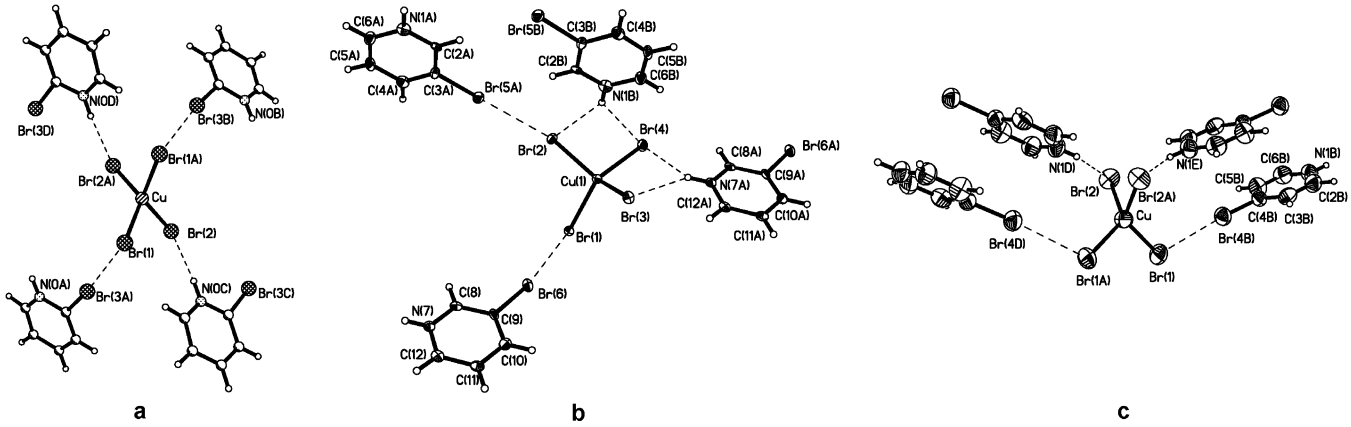

Figure 1. Synthon interactions in (a) 2BP−Br, (b) 3BP−Br, and (c) 4BP−Br.

Table 1. Selected Bond Distances and Angles

crystal	$(2BP)_2CuBr_4$	$(3BP)_2CuBr_4$	$(4BP)_2CuBr_4$	$(2BP)_2CuCl_4$	$(3BP)_2CuCl_4$	$(4BP)_2CuCl_4$
trans angle 1	133.34 (6)	135.73(6)	128.44(4)	130.40(5)	144.65(6)	134.06(7)
trans angle 2		133.97(6)			139.71(7)	133.79(7)
Cu−X1 distance	2.371 (1)	2.372(2)	2.352(2)	2.174(1)	2.295(2)	2.254(2)
Cu−X2 distance	2.407 (2)	2.384(2)	2.391(2)	2.259(1)	2.229(2)	2.267(2)
Cu−X3 distance		2.392(2)			2.238(1)	2.236(2)
Cu−X4 distance		2.394(2)			2.230(1)	2.219(2)

molecular interaction in determining crystalline structure in this series of compounds.

Structure Descriptions

The crystal structures all consist of isolated, planar bromopyridinium cations and distorted tetrahedral CuX_4^{2-} anions. Of the three $(n\text{BP})_2CuX_4$ pairs, X = Cl and Br, only the $2BP^+$ salts are isomorphous. The anions all exhibit the typical flattened tetrahedral geometry with approximate D_{2d} symmetry, although the extent of flattening is not large. The average trans X−Cu−X angles are in the range 128.4−134.8° for the bromide salts and 130.4−142.2° for the chlorides. The smaller values of these trans angles are in the range normally observed for salts containing non-hydrogen bonding cations. The exceptions are the larger trans angles in the 3BP−Cl salt, where a bromine atom from one of the pyridinium cations packs so as to form a close contact (4.005 Å) with the copper atom, forcing one of the trans angles further open.

A variety of supramolecular interactions tie the anions and cations together in these structures. The structures will be analyzed in the following sequence: (a) examination of the environment of the pyridinium cation and CuX_4^{2-} anions to identify the significant C−Br···X^- and N−H···X^- interactions; (b) description of the resultant supramolecular networks; (c) analysis of the stacking interactions between cations and the resultant three-dimensional structures of the compounds. It will be seen that diverse stacking interactions between cations occur in the six compounds examined, with both linear and bifurcated N−H···X^- hydrogen bonds being found. Most significantly, it will be seen that short, nearly linear C−Br···X^- interactions occur in all cases. The dominant features in these six structures are the presence of these C−Br···X^- contacts and of hydrogen bonding interactions between the pyridinium N−H^+ group and the copper(II) halide species. The supramolecular interactions link the cationic and anionic species into a variety of chains or, in one case, layer substructures. These substructures are then aggregated into the final three-dimensional crystals via stacking interactions between the cations and other weaker supramolecular interactions (C−H···X^- contacts, 90° C−Br···X^- and C−Br···Br−C contacts, etc).

C−Br···X^- and N−H···X^- Interactions. The environments of the bromopyridinium cations, shown in Figure 1 for the three $CuBr_4^{2-}$ salts, illustrate the geometric nature of the linear C−Br···Br^- and of the N−H···Br^- contacts. The data summarizing these contacts are tabulated in Table 2 for all six compounds. The Br···Br^- distances range from 3.390 to 3.449 Å, considerably shorter than the sum of the van der Waals radii (3.80 Å), and the C−Br···Br^- angles range from 169.5 to 179.0°. For the compounds containing $CuCl_4^{2-}$ anions, the corresponding Br···Cl^- distances and C−Br···Cl^- angles range from 3.271 to 3.358 Å and from 167.0 to 178.8°, respectively. Thus, the Br···X^- contacts are roughly 0.30−0.40 Å shorter than the sum of the van der Waals radii. In addition to the short linear C−Br···X^- interactions, numerous other C−Br···X^- interactions occur with distances greater than 3.9 Å (X = Br) and 3.75 Å (X = Cl). The shortest of these 90° interactions are also given in Table 2. Also, in two instances, 90−90° interactions are observed between arylbromines on adjacent cations.

Examination of the N−H···X^- interactions reveal three different hydrogen bonding patterns: linear N−H···X^- (in 2BP−X, 2BP−Cl, and 4BP−Cl), symmetric bifurcated interactions (in 3BP−Br and 4BP−Cl) and asymmetric bifurcated interactions (in 4BP−Br, 3BP−Cl, and 4BP−Cl). Thus, while strong hydrogen bonding interactions occur in all cases, a variety of conformations that achieve these interactions are observed. In the corresponding (*n*-methylpyridinium)$_2CuBr_4$ salts, linear and symmetric bifurcated hydrogen bonds are reported, but not the asymmetric bifurcated bonds. This would indicate that the

Table 2. C−Br···X and N−H···X Synthon Distances and Angles in the *n*BP$^+$ Salts

compound[a]	Br···X(Å)[b]	C−Br···X(°)	X···Br−Cu(°)	N···X(Å)	H···X(Å)	N−H···X(°)	type of H-bond
$(2BP)_2CuBr_4$	3.449	174.2	96.8	3.159	2.299	173.8	linear
	*3.956**	*110.0*					
$(3BP)_2CuBr_4$-cat1	3.390	179.0	119.8	3.425	2.684	142.6	bifurcated
				3.567	2.869	137.4	
-cat2	3.397	168.5	142.6	3.404	2.642	137.2	bifurcated
	3.947	*70.0*		3.341	2.699	138.0	
$(4BP)_2CuBr_4$	3.435	174.7	114.9	3.370	2.259	145.5	asym bifurcated
	3.976	*90.1*		3.561	2.881	149.2	
	3.899	*80.5*					
	*3.966**	*95.2*					
$(2BP)_2CuCl_4$	3.322	175.8	94.1	2.296	2.078	169.0	linear
$(3BP)_2CuCl_4$-cat1	3.283	174.5	169.0	3.321	2.624	139.4	bifurcated
				3.182	2.472	140.4	
-cat2	3.271	167.0	158.3	3.149	2.347	155.5	asym bifurcated
	3.876	*76.4*		3.334	2.899	113.3	
	3.735	*95.9*					
$(4BP)_2CuCl_4$	3.356	173.8	126.0	3.121	2.344	150.4	asym bifurcated
					2.825	128.7	
	3.358	178.8	100.1	3.094	2.269	160.7	linear
	3.844	*128.6*					

[a] When two crystallographic cations are present, they are denoted by cat1 or cat2. [b] The most significant C−Br···X 90° interactions are given in italics. Those denoted with an asterisk are C−Br···Br−C interactions.

Scheme 1

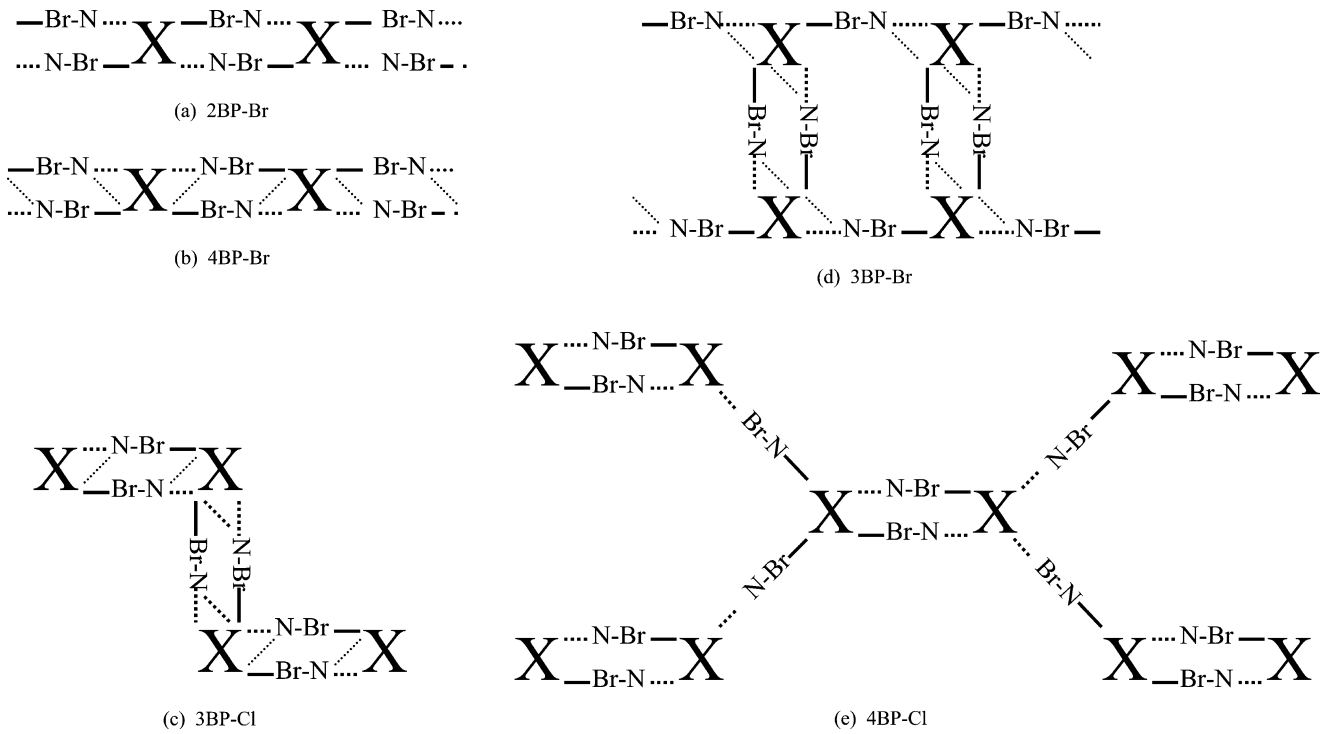

presence of the linear supramolecular C−Br···Br$^-$ interactions causes significant perturbations on the packing of the cationic and anionic species in these materials.

Description of the Supramolecular Networks. As a consequence of these C−Br···X$^-$ interactions, the presence of a Br substituent on the pyridine ring transforms the pyridinium cation from a monofunctional synthon into a bifunctional synthon (ignoring the less well-defined stacking interactions). Thus, the crystal structures of the CuX_4^{2-} salts of the bromopyridinium cations possess well-defined extended $[(CuX_4^{2-})(nBP^+)_2]_n$ networks. These can then aggregate into the final crystal structure via stacking interactions between the cations as well as other weaker supramolecular interactions. This is in contrast to the alkyl-substituted pyridinium complexes, where simple hydrogen bonded $(CuX_4^{2-})(spyH^+)_2$ units are formed that aggregate into extended networks via $\pi-\pi$ stacking interactions.

The extended networks developed by the combinations of N−H···X$^-$ and C−Br···X$^-$ synthons are illustrated schematically in Scheme 1. Here the CuX_4^{2-} anion is designated by the "x" while bromopyridinium cation is simply represented by "Br−N". The linear C−Br···X$^-$ interactions are denoted by solid lines, while the N−H···X$^-$ interactions (either linear or bifurcated) are represented by dotted lines (lighter dotted lines denote the weaker half of an asymmetric hydrogen bond). Of the six compounds reported in this study, four form chain networks, one forms a double chain network, and the final one forms a two-dimensional network.

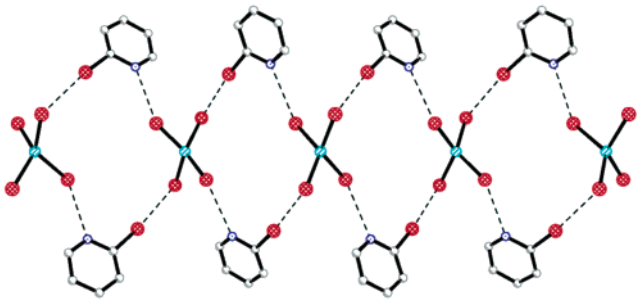

Figure 2. Chain network in 2BP−Br, showing the C−Br···Br^- and N−H···Br^- synthonic interactions. The chains run parallel to the *c* axis.

Present in all of the networks are bibridged [CuX_4^{2-} − (nBP^+)$_2$ − CuX_4^{2-}] units. In addition, the more complex schemes of the double chain network and the two-dimensional network incorporate monobridged [CuX_4^{2-} − (nBP^+) − CuX_4^{2-}] units. The C−Br···X^- synthons are essentially linear in all cases, but the N−H···X^- synthons take on any one of the three hydrogen bonding schemes described above: linear, symmetric bifurcated, or asymmetric bifurcated. The fact that the chloride and bromide salts for the $3BP^+$ and $4BP^+$ cations are not isomorphous indicates that other interactions, beyond those involving in the two synthons, play subtle but significant roles in determining the ultimate geometry of the networks. This is perhaps not due so much to the variability in the geometry of the synthonic N−H···X^- and C−Br···X^- interactions, but rather the variation of the Cu−X···X and Cu−X···H angles. For example, the Cu−Br···Br angles in 3BP−Br are 119.8 and 142.6°, while the Cu−Cl···Br angles in 3BP−Cl are 158.3 and 169.0°.

The chain networks observed in the 2BP−X (Scheme 1a) and 4BP−Br (Scheme 1b) structures are topologically similar, although the differences in their geometric nature yield drastically different structural characteristics. A very open network is developed in the structure of 2BP−Br, where the linear N−H···X^- synthon (Figure 2) is found. Each bromide ion of a given $CuBr_4^{2-}$ anion is involved in only one synthonic interaction. The chains run parallel to the (0 0 1) direction, with adjacent anions in the chain related by unit cell translation. This gives closest contacts between anions of 4.578 Å. The presence of the Br substituent in the 2-position leads to a very acute bridging angle between adjacent $CuBr_4^{2-}$ tetrahedra and prevents stacking of the cations within the chain network. In contrast, the chain in the 4BP−Br salt is much more compact, since the *para* substitution allows pairs of coplanar $4BP^+$ cations to link adjacent anions. Each bridging pair of $4BP^+$ cations stack in an antiparallel fashion so that the Br atom of one cation overlaps the pyridinium ring of the second one in the bridge. In this manner, zigzag chains, as shown in Figure 4, are formed that run parallel to (1 0 $\bar{1}$). In this structure, the N−H···X^- synthons now exhibit very asymmetric bifurcated hydrogen bonds. For the anions, the bromide ions on the exterior of the chain are involved in the C−Br···Br^- synthonic interactions (as well as in the weaker leg of the bifurcated hydrogen bonds), while the inner pairs of bromide ions are involved in the stronger leg of the bifurcated hydrogen bonds. The chains in 3BP−Cl (Scheme 1c) are topologically different than the previous two chains, in that one of the halide ions in each of the CuX_4^{2-} anions is not involved in synthon formation. These chains, that run parallel to the (1 1 $\bar{1}$) direction, contain two alternating, but very similar, bridging arrangements (Figure 3). The main difference is that the bifurcated hydrogen bonds for cation 1 are nearly symmetric, but they are quite asymmetric for cation 2. In both cases, one of the chloride ions involved in the bifurcated hydrogen bond is also the recipient of the C−Br···Cl^- interaction.

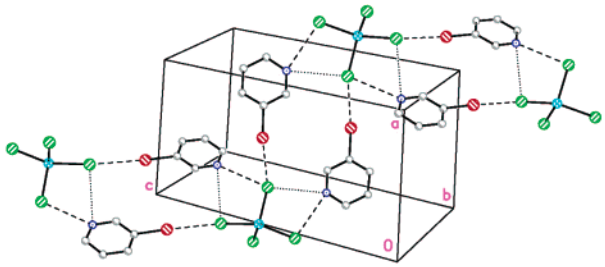

Figure 3. Chain network in 3BP−Cl, showing the C−Br···Cl^- and asymmetric bifurcated N−H···Cl^- synthonic interactions. The weaker link in each of the bifurcated hydrogen bonds is denoted by dotted lines. The chains run parallel to the (1 1 $\bar{1}$) direction. Type 1 cations form the bibridged units that lie horizontal while type 2 cations form vertical linkages.

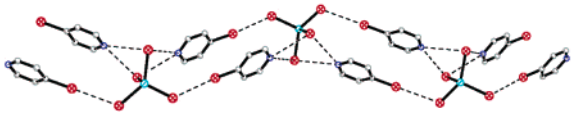

Figure 4. Chain network in 4BP−Br, showing the C−Br···Br^- and N−H···Br^- synthonic interactions. The chains run parallel to the (1 0 $\bar{1}$) direction.

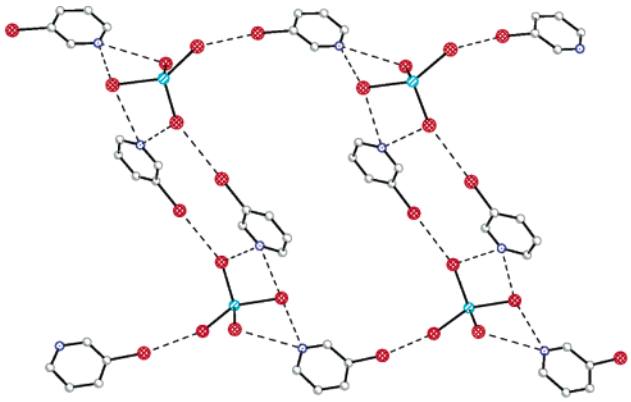

Figure 5. Ladder chain network in 3BP−Br, illustrating the existence of both monobridged and bibridged [$CuBr_4^{2-}$ − (nBP^+)$_n$ − $CuBr_4^{2-}$] synthonic interactions. The chains run parallel to the (1 0 $\bar{1}$) direction.

These three single strand chains only contain bibridged [CuX_4^{2-} − (nBP^+)$_2$ − CuX_4^{2-}] units, although the position of the Br substitution dramatically affects the geometry in the bibridged pairs. In the more complex double chain in 3BP−Br and the two-dimensional network of 4BP−Cl, both bibridged and monobridged units occur. Nevertheless, the nature of the bibridged units found in the chain networks is retained. Figure 5 illustrates the double chain network in 3BP−Br that runs parallel to the (1 1 $\bar{2}$) direction. This network can be viewed as a ladder network (Scheme 1d), with the

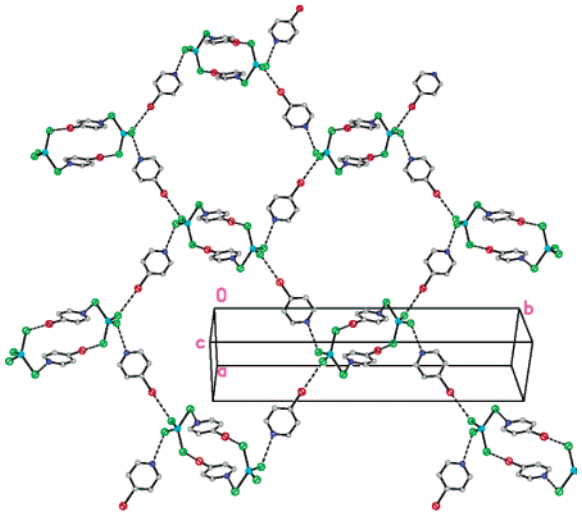

Figure 6. Two-dimensional network in 4BP−Cl, illustrating the existence of both monobridged and bibridged $[CuCl_4^{2-} - (nBP^+)_n - CuCl_4^{2-}]$ synthonic interactions. The networks lie parallel to the (2 0 $\bar{1}$) planes.

monobridged linkages making up the rails and the bibridged linkages defining the rungs. Bifurcated hydrogen bonds are formed in both bridging arrangements, with the weaker link of the bifurcations being directed toward the one common bromide ion. The complex two-dimensional network found in 4BP−Cl (Scheme 1e) consists of bibridged $[CuX_4^{2-} - (4BP^+)_2 - CuX_4^{2-}]$ units linked to four neighboring units by monobridging $4BP^+$ cations, as illustrated in Figure 6. The bibridged units are similar to those found in 4BP−Br, with strongly asymmetric bifurcated hydrogen bonds. The stacking of the two $4BP^+$ cations in the bibridged arrangement is also essentially identical to that found in 4BP−Br, with the Br^- atom of one cation roughly lying above the ring of the second cation. In the monobridging unit, the hydrogen bond is not bifurcated, but nevertheless is distorted 20° from linearity.

Table 3. Cation Stacking Interactions

compound	cation	$d_\perp$ (Å)	d_{x-x} (Å)	Φ (°)	d_{x-Br} (Å)	Φ′ (°)
$(2BP)_2CuBr_4$		3.538	4.028	28.6		
$(3BP)_2CuBr_4$	1	–	–	–		
	2	3.200	4.071	38.2		
$(4BP)_2CuBr_4$		3.568	4.562	38.8	3.637	12.7
$(2BP)_2CuCl_4$		3.523	3.800	22.0		
$(3BP)_2CuCl_4$	1	3.541	3.639	13.3		
	2	3.535	3.819	22.2		
$(4BP)_2CuCl_4$	1	3.550	4.171	31.7	3.774	19.7
	2	–	4.634	40.8, 41.6	3.519	2.9

Stacking Interactions and Final Crystal Structures. Two different types of packing interactions exist between the pyridinium cations: (a) normal $\pi-\pi$ stacking, found with the $2BP^+$ and $3BP^+$ cations, and (b) π−Br stacking interactions observed with $4BP^+$ cations. Table 3 gives a summary of the stacking arrangements between cations in the final structures of the compounds, while Figure 7 gives representative illustrations of the stacking of adjacent cations in the final structures as viewed perpendicular to the cation plane. The parameters defined in Table 3 are (a) $d_\perp$, the perpendicular distances between cation planes (only defined when the planes are parallel), (b) d_{x-x}, the centroid to centroid distance between adjacent pyridinium rings, (c) Φ, the angle between the line between centroids and

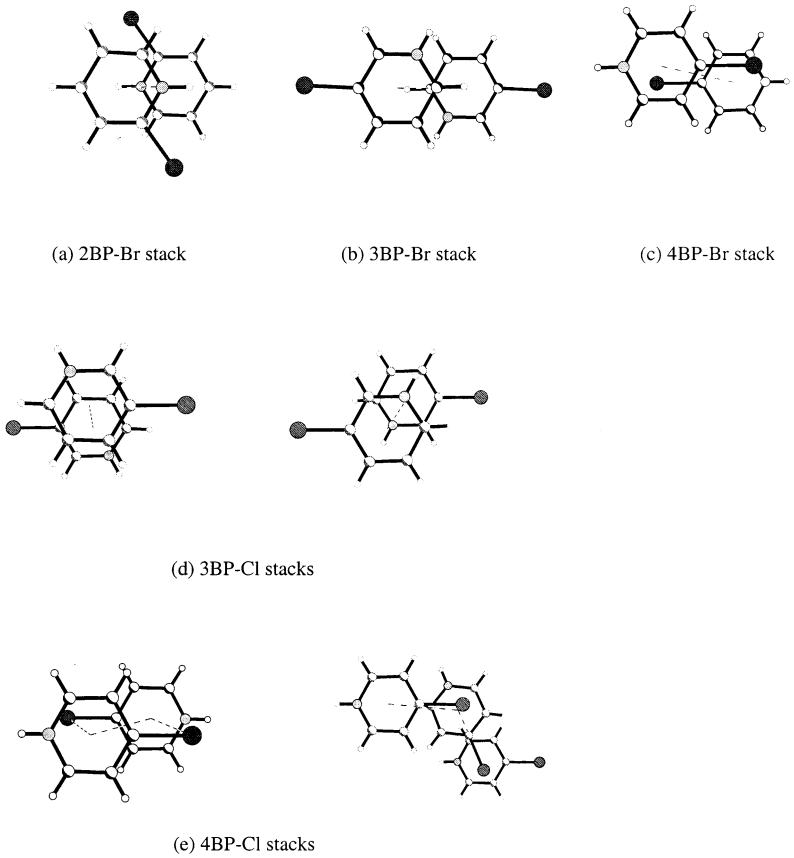

Figure 7. Illustration of the $\pi-\pi$ and π−Br stacking arrangements for the cations. Views are from the normal to the planes of the cations. The dashed lines denote centroid−centroid or centroid−bromine connections.

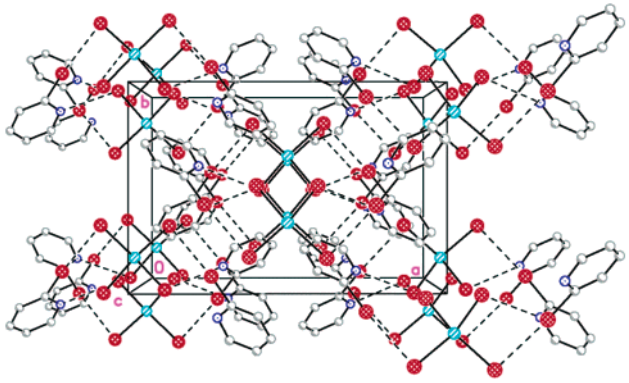

Figure 8. Illustration of the stacking of the pyridinium rings in the 2BP−Br structure. The view is parallel to the chain directions, with chains located at cell corners and the center of the *bc* face.

the normal to the plane of the cation, (d) d_{x-Br}, the centroid to bromine distance in adjacent cations and (e) Φ′, the angle between the centroid−bromine line and the normal to the plane of the cation.

It is clear that overall no real systematics occur in the stacking interactions, although some patterns are seen for each type of nBP$^+$ cation. This is particularly true for the 4BP$^+$ cation, where significant π−Br stacking interactions occur, as seen in Figure 7c,e. Here the bromine atom from one cation lies above the ring of an adjacent cation. This leads to a large d_{x-x} distance (> 4 Å) and a Φ angle greater than 30°. With the 2BP$^+$ and 3BP$^+$ cations, some π−π overlap between pyridine rings occurs, but only for the cations in 3BP−Cl (Figure 7d) is there substantial overlap of the pyridinium rings. For the 2BP−X and 3BP−Br structures, the rings barely overlap (Figure 7a,b). In fact, for cation 1 in 3BP−Br, no significant stacking interactions occur. The aggregation of these networks into the final crystal structures appears to be largely controlled by these supramolecular stacking interactions between the nBP$^+$ cations and to other weaker supramolecular interactions, such as C−H···X contacts, 90° C−Br···X contacts, etc. This is in contrast to the *N*-alkyl substituted pyridinium salts, where hydrogen bonded [(CuX_4^{2-})(nBP$^+$)$_2$] monomer units are weakly aggregated into chains through π−π stacking interactions.[12]

Examination of the overall crystal structures reveal that the extent to which the stacking interactions play a significant role in the overall structure largely depends on the accessibility of the pyridinium rings in the supramolecular networks described above. Thus, intranetwork stacking interactions are found to be more important in the open structure of the 2BP−X salts, for example, than in the very compact structure found for 4BP−Br. In the chain structure for 2BP−Br (Figure 2), where the nBP$^+$ cations protrude out from the chain, they partially interdigitate between cations on adjacent chains, as illustrated in Figure 8, effectively locking the chains together. Thus, the supramolecular π−π stacking interactions play a significant role in the determination of the final structure. In contrast, the compact 4BP−Br chains (Figure 4) aggregate into layers (Figure 9) with only minimal interactions between chains. No additional stacking of the cations exists, beyond the π−Br stacking within the bibridged units in the chains.

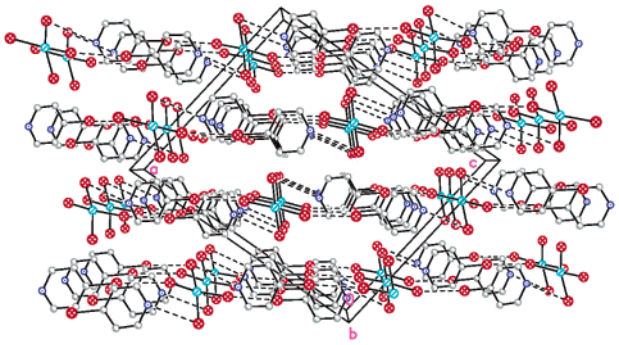

Figure 9. Illustration of stacking of chains in 4BP−Br into layers lying parallel to (1 0 1).

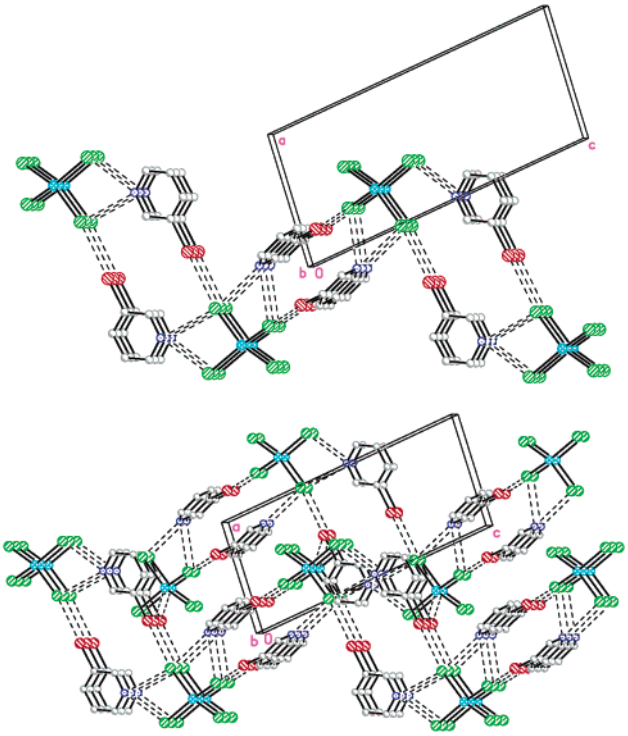

Figure 10. (a) Illustration of the stacking of chains in 3BP−Cl to form layers lying parallel to (1 0 1). (b) Interleaving of anions and cations in adjacent layers.

The layers lie parallel to the (1 0 1) planes, with only weak 180−90° C−Br···C−Br interactions holding the chains together into the layers and with weak 90° C−Br···Br$^-$ and C−H···Br$^-$ contacts between layers.

The 3BP$^+$ structures are intermediate between the above two extremes. Both the chloride and bromide salts contain two independent cations, only one of which is involved with internetwork stacking interactions. In the zigzag network observed for 3BP−Cl (Figure 3), stacking of the pyridinium rings centered about the unit cell origins tie the chains together into sheets lying in the (1 0 1) planes, as seen in Figure 10. Adjacent sheets interleave, with the $CuCl_4^{2-}$ anions of one sheet interdigitating between cations of the second type on an adjacent sheet. For 3BP−Br, the ladder networks (Figure 5) stack atop each other along the *a* direction, with the $CuBr_4^{2-}$ anions on a given ladder interdigitating between cations from the bibridged units on the next ladder. Then the monobridged cations of the edges of

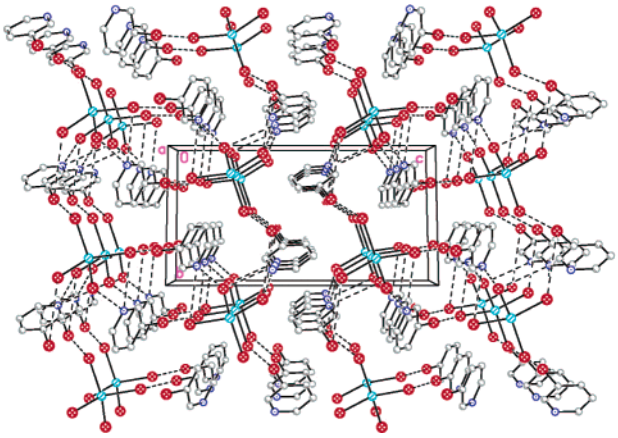

Figure 11. Illustration of the layers formed from the double chains in 3BP−Br. Individual chains run parallel to the *b* axis, with the layers lying in *ab* planes. $\pi-\pi$ stacking interactions tie the layers together.

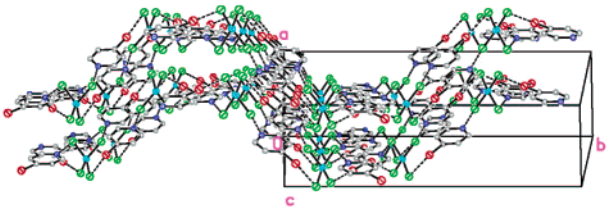

Figure 12. Illustration of the nesting of layers in 4BP−Cl.

these columns form $\pi-\pi$ stacks with their neighboring columns to develop the final three-dimensional structure (Figure 11).

Finally, in the two-dimensional sheet structure for 4BP−Cl (Figure 6), the networks nest as shown in Figure 12. The two crystallographically independent cations contribute in significantly different ways to the development of the structure. For cation 1, involved in the $\pi-$Br interactions in the double bridges within the layer, no significant stacking occurs between layers. In contrast, the monobridging cation, cation 2, there is significant $\pi-$Br stacking between layers. This stacking develops the undulating stacks of cations running parallel to (1 0 $\bar{1}$).

Discussion

The results reported here clearly show the significance of aryl C−Br···X^- synthons in the determination of the supramolecular structure of tetrahalocuprate(II) salts. In the studies of Luque et al.[17] on the methyl and ethyl substituted pyridinium salts, it was the presence of $\pi-\pi$ stacking that complimented the major N−H···X^- hydrogen bonding interactions and led to chain structures based on alternating hydrogen bonding/$\pi-\pi$ stacking interactions. In the compounds reported here, it is the C−Br···X^- synthons that cooperate with the hydrogen bonding to yield low dimensional networks. The role of $\pi-\pi$ stacking, when present, is to facilitate the packing of these networks into the final three-dimensional structure.

To further substantiate these results, we have examined the structures of the bromocuprate(II) salts of various bromo-substituted 2-aminopyridinium or 2,6-diaminopyridinium cations reported in the literature. The structural parameters for the major interactions involving the aryl C−Br moieties are summarized in Table 4. In these compounds, the presence of an amino group in the *ortho* position gives the pyridinium cation the potential to hydrogen bond in a concerted bidentate-type fashion, with the pyridinium N−H and an amino N−H groups typically hydrogen bonding to two bromide ions on a CuX_4^{2-} anion. Thus, with the 2:1 cation/anion ratio, all four halide ions are usually strongly involved in hydrogen bonding. Nevertheless, the results given in Table 4 confirm that these aryl C−Br···X^- interactions often play an important role, but also points to their limitations when competing with cations that have more extensive hydrogen bonding capabilities. Significantly, in some cases, the type I C−Br···Br−C synthon is found in addition to, or instead of, the linear C−Br···Br^- synthon. Also, a new version of the C−Br···Br^- synthon is observed, in which a bifurcated interaction with two bromide ions occurs.

One interesting series of compounds is found in the structures of $(3MAP)_2CuBr_4$,[19] (3MAP)(5B3MAP)$CuBr_4$,[20] and $(5B3MAP)_2CuBr_4$,[21] where 3MAP is the 3-methyl-2-aminopyridinium cation and 5B3MAP is the 5-bromo-3-methyl-2-aminopyridinium cation. The crystal structures of these three compounds are all different, as might be anticipated on steric grounds when the large bromine atom is substituted for a hydrogen atom on the pyridine ring. When one 3MAP cation is replaced by a 5B3MAP cation, a linear C−Br···Br^- interaction is found, with a distance of 3.483 Å and an angle of 176.2°. Thus, the aryl C−Br···Br^- synthon competes well

Table 4. C−Br···Br^- and C−Br···Br−C Synthon Distances and Angles in Other Bromocuprate(II) Salts[a]

compound[b]	Br···Br^- (Å)[c]	C−Br···Br^- (°)	C−Br···Br−C (Å)	C−Br···Br^- (°)	ref
(3MAP)(5B3MAP)$CuBr_4$-I					20
-II	3.502	174.6			
$(5B3MAP)_2CuBr_4$-I	3.568	160.6			21
-II			3.561	144.5	
$(5BAP)_2CuBr_4$			3.393	156.5	24
$(35DBAP)_2CuBr_4$-IA	3.530	162.8			26
-IB	3.447	167.3			
-IIA	3.808	97.1	3.863, 3.879	118.8, 103.0	
-IIB	3.632,3.714	147.1, 142.4			
$(4B3HAP)_2CuBr_4$	3.540	161.8			
$(35DB26DAP)_2CuBr_4$-A			3.673	130.3	22
-B	3.506	171.5			
(AP)Cu(5bap)Br_3	3.773	171.9			27

[a] Acronyms: 3MAP = 3-methyl-2-aminopyridinium; 5B3MAP= 5-bromo-3-methyl-2-aminopyridinium; 5BAP = 5-bromo-2-aminopyridinium; 35DBAP = 3,5-dibromo-2-aminopyridinium; 4B3HAP = 4-bromo-3-hydroxy-2-aminopyridinium; 35DB26DAP = 3,5-dibromo-2,6-diaminopyridinium; AP = 2-aminopyridinium, 5bap = 5-bromo-2aminopyridine. [b] Different cations in the structure are denoted by the symbols I or II. Multiple bromine atoms on a cation are denoted by A or B. [c] Two entries indicate the presence of a bifurcated interaction.

Table 5. Summary of Data Collection and Refinement Parameters

crystal	2BP−Br	3BP−Br	4BP−Br	2BP−Cl	3BP−Cl	4BP−Cl
formula	$C_{10}H_{10}Br_6CuN_2$	$C_{10}H_{10}Br_6CuN_2$	$C_{10}H_{10}Br_6CuN_2$	$C_{10}H_{10}Br_2Cl_4CuN_2$	$C_{10}H_{10}Br_2Cl_4CuN_2$	$C_{10}H_{10}Br_2Cl_4CuN_2$
formula weight	701.20	701.20	701.20	523.36	523.36	523.36
D_{calc} (mg/m^3)	2.50	2.632	2.555	2.028	2.098	2.044
T (K)	295	81	295	295	295	295
crystal system	monoclinic	triclinic	monoclinic	monoclinic	triclinic	monoclinic
space group	*C*2/*c*	*P*-1	*C*2/*c*	*C*2/*c*	*P*-1	$P2_1/c$
a (Å)	14.519(5)	6.501(2)	16.904(2)	12.938(5)	7.5639(9)	7.7752(9)
b (Å)	9.674(2)	8.573(3)	7.766(1)	12.938(5)	7.815(1)	27.963(3)
c (Å)	13.304(4)	16.192(6)	14.029(2)	12.938(5)	15.544(2)	8.723(1)
α (°)	90	89.76(7)	90	90	82.11(1)	90
β (°)	91.12(3)	89.67(9)	98.19(1)	12.938(5)	78.87(1)	116.251(7)
γ (°)	90	78.70(8)	90	90	67.060(8)	90
V (Å^3)	1868.1(9)	884.8(5)	1822.9(4)	1714(1)	828.3(2)	1701.0(3)
ind. reflections	1232	4393	1598	1502	2907	3008
R (int)		0.0776	0.0482	0.0443	0.0383	0.0515
Z	4	2	4	4	2	4
goodness of fit	1.172	0.951	1.043	1.089	1.067	1.025
R_1[a] [$I > 2\sigma$]	0.0457	0.0509	0.0570	0.0388	0.0377	0.0441
wR_2[b] [$I > 2\sigma$]	0.0553	0.0840	0.1284	0.1060	0.0853	0.0873
μ (mm^{-1})	13.88	14.769	14.338	6.546	6.774	6.597
trans range	0.242−0.520	0.320−0.590	0.057−0.154	0.882−1.216	0.279−0.416	0.314−0.386

[a] $R_1 = \sum||F_o| - |F_c||/\sum|F_o|$. [b] $wR_2 = \sum w||F_o|^2 - |F_c|^2|/\sum w|F_o$.

with the hydrogen bonding. However, when both 3MAP cations are replaced by their 5B3MAP analogues, this is no longer the case. One of the cations still participates in a C−Br···Br$^-$ synthon, but the distance is longer (3.568 Å) and the angle deviates more from linearity (160.6°). More significantly, the second set of cations form type I short, symmetric C−Br···Br−C contacts with Br···Br distances of 3.561 Å and a C−Br···Br angle of 144.5°. Thus, their multiple hydrogen bonding capabilities overcome the attraction of the C−Br group for the bromide ion, and the C−Br···Br−C synthon is utilized instead. A similar situation is also found to occur in the 3,5-dibromo-2-aminopyridinium salt, $(35DBAP)_2CuBr_4$, where one of the bromine atoms in the cation is involved in a C−Br···Br$^-$ synthonic interaction while the second forms an C−Br···Br−C synthon with a neighboring cation.[22]

A more intriguing case where the C−X···X−C synthon is found occurs in the $(5XAP)_2CuBr_4$ series, where X = methyl (5MAP),[23] chlorine (5CAP),[24] bromine (5BAP),[24] or iodine (5IAP)[25]. In this series, the first three salts are isostructural, but the iodide derivative crystallizes as a dihydrate and assumes a new structure. The structures of the first three are stabilized by a set of strong hydrogen bonds and an efficient $\pi-\pi$ stacking arrangement. In these three, the 5XAP cations align so that short C−X···X−C contacts are formed, with the X···X distances being 3.734, 3.303, and 3.393 Å for X = Me, Cl, and Br, respectively, while the C−X···X angles are 164.8, 156.8, and 156.5° respectively. In the 5MAP salt, the shortness of the C−CH_3 bond allows the cations to pack in the observed fashion without undo repulsive interactions between the methyl groups. For the 5CAP and 5BAP salts, the development of the type I C−X···X−C synthon helps stabilize the structure. However, the structure forces a very short X···X distance, with an increase of only 0.09 Å upon going from the chlorine to the bromine derivative. It is clear that the structure does not have sufficient flexibility to accommodate the larger iodide ion, so the 5IAP derivative must assume a different structure.

Finally, the 3,5-dibromo-2-aminopyridinium salt, $(35DBAP)_2CuBr_4$,[26] provides an example of a bifurcated C−Br···Br$^-$ synthon. The structure contains two crystallographically independent cations, so there are four possible synthonic interactions involving the aryl bromine atoms. Two form normal short, linear C−Br···Br$^-$ contacts (see Table 4) while a third is only involved in relatively weak 180−90° interactions. The fourth bromine forms the bifurcated synthon, with the two bromide ions at a distance of 3.632 and 3.714 Å, with angles of 147.1 and 142.4°, respectively. A bifurcated interaction is also found in (2AP)Cu(5b2ap)Br_3, where 2AP is the 2-aminopyridinium cation and 5b2ap is neutral 5-bromo-2-aminopyridine.[27]

In summary, these studies clearly show the importance of the C−Br···X$^-$ synthon in determining the supramolecular structure of the tetrahalocuprate(II) salts. In subsequent papers, we will examine the role of the C−Br···X$^-$ synthons in the structures of the tetrahalocuprate(II) salts and other halometalate salts with various dibromopyridinium cations, as well as the structures of complexes with the neutral ligands.

Experimental Section

Synthesis and Crystal Growth. (a) Bis(2-bromopyridine)tetrabromocuprate(II), 2BP−Br. A total of 1 mmol of 2-bromopyridine and 1 mmol of copper(II) bromide were dissolved in 15 mL of 95% ethanol acidified with 5 mL of concentrated hydrobromic acid. The solution was heated and stirred for 30 min. Crystals developed from the solution at room temperature after several days. A dark brown crystal with dimensions 0.3 × 0.3 × 0.2 mm was used for the structure determination.

(b) Bis(3-bromopyridinium)tetrabromocuprate, 3BP−Br. A total of 1 mmol of 3-bromopyrodine and 1 mmol of copper(II) bromide were refluxed in 15 mL of nitromethane acidified with 5 mL of concentrated hydrobromic acid solution. The solution was left uncovered to evaporate. Dark brown crystals developed in few days. The crystals turned green when

exposed to moist air and became amorphous. A fragment of 0.10 × 0.06 × 0.04 mm was used for the structure determination.

(c) Bis(4-bromopyrdinium)tetrabromocuprate(II), 4BP−Br. A total of 1 mmol of 4-bromopyridine hydrochloride and 1 mmol of copper(II) bromide were dissolved in 5 mL of absolute ethanol acidified with 1 mL of concentrated hydrobromic acid and warmed to 70 °C for 30 min. The volume of the solution was reduced on warm hotplate in a current of dry air. Large dark brown mostly flat crystals developed. Data collection was finally done on a single crystal with dimensions 0.28 × 0.25 × 0.08 mm coated with epoxy to reduce air exposure.

(d) Bis(*n*-bromopyridinium)tetrachlorocuprate salts, 2BP−Cl, 3BP−Cl, and 4BP−Cl. The general procedure, with small variations between various preparations, is as follows: 1 mmol of the brominated pyridine and 1 mmol of copper(II) chloride dihydrate were dissolved in 15 mL of absolute ethanol methanol that had been acidified with 2 mL of concentrated hydrochloric acid. The mixture was heated and stirred in a small covered beaker for 1 h. Large yellow needle crystals developed at room temperature in 1−3 days. Crystals of appropriate size were cut from larger crystals for the structure determinations.

Crystal Structure Determinations. The crystal structure of 3BP−Br was determined at 81 K with the remainder determined at room temperature. The data collection for 2BP−Br was carried out on a Nicolet R3m/E system.[28] The orientation matrix and lattice parameters of the triclinic crystals were optimized from the least-squares refinement to the angular settings of 25 carefully centered reflections with high Bragg angles. The SHELXTL 4.1 software package was used for data reduction and refinement.[29] For 4BP−Br, 2BP−Cl, 3BP−Cl, and 4BP−Cl, a Syntex $P2_1$ diffractometer upgraded to Bruker P4 specifications was utilized. Lattice dimensions were obtained from 25 accurately centered high angle reflections.[30] Data were corrected for absorption utilizing psi scan data assuming an ellipsoidal shaped crystal. Structure solutions and refinement were obtained using the SHELXTL package.[31] Finally, the data for 3BP−Br were collected on a Bruker 3-circle platform diffractometer equipped with a SMART APEX CCD detector. The frame data were acquired with the SMART[32] software using MoKα radiation (λ = 0.71073 Å). The frames were then processed using the SAINT software[33] to give the *hkl* file corrected for Lp/decay. The absorption correction was performed using the SADABS[34] program. The structure was solved and refined by least-squares method on F^2 with the SHELXTL package.[31] Hydrogen atoms for all structures were included at calculated positions. Data collection parameters and refinement results are given in Table 5.

Acknowledgment. This research was supported by ACS-PRF 34779-AC5.

Supporting Information Available: Crystal data for all six compounds in CIF format. This material is available free of charge via the Internet at http://pubs.acs.org.

References

(1) (a) Desiraju, G. R. *Nature* **2001**, *412*, 397. (b) Desiraju, G. R. *Curr. Sci.* **2001**, *81*, 1038.
(2) Aakeröy, C. B.; Beatty, A. M. *Aust. J. Chem.* **2001**, *54*, 409.
(3) Garden, S. T.; Fontes, S. P.; Wardell, J. L.; Skakle, J. M.; Low, J. N.; Glidewell, C. *Acta Crystallogr.* **2002**, *B58*, 701.
(4) (a) Reddy, D. S.; Craig, D. C.; Rae, A. D.; Desiraju, G. R. *J. Chem. Soc., Chem. Commun.* **1993**, 1737. (b) Bailey, R. D.; Hook, L. L.; Watson, R. P.; Hanks, T. W.; Pennington, W. T. *Cryst. Eng.* **2000**, *3*, 155. (c) Walsh, R. B.; Padgett, C. W.; Metrangolo, P.; Resnati, G.; Hanks, T. W.; Pennington, W. T. *Cryst. Growth Des.* **2001**, *1*, 165.
(5) (a) Lommerse, J. P. M.; Stone, A. J.; Taylor, R.; Allen, F. *J. Am. Chem. Soc.* **1996** *118*, 3108. (b) Xu, K.; Ho, D. M.; Pascal, R. A. *J. Am. Chem. Soc.* **1994**, *116*, 105. (c) Schmidt, G. M. J. *Pure Appl. Chem.* **1971**, *27*, 647. (b) Dunitz, J. D.; Taylor, R. *Chem. − Eur. J.* **3**, *89*. (d) Howard, J. A. K.; Hoy, V. J.; O'Hagen, D.; Smith, G. T. *Tetrahedron* **1996**, *52*, 12613. (e) Broder, C. K.; Howard, J. A. K.; Keen, D. A.; Wilson, C. C.; Allen, F. H.; Jetti, R. K. R.; Nangia, A.; Desiraju, G. R. *Acta Cryst.* **2000**, *B56*, 1080.
(6) (a) Price, S. L.; Stone, A. J.; Lucas, J.; Rowland, R. S.; Thornley, A. E. *J. Am. Chem. Soc.* **1994**, *116*, 4910. (b) Murray, J. S.; Paulson, K.; Polizer, P. *Proc. Ind. Acad. Sci. (Chem. Sci.)* **1994**, *118*, 3108. (c) Jetti, R. K. R.; Xue, F.; Mak, T. C. W.; Nangia, A. *Cryst. Eng.* **1999**, *2*, 214. (d) Jetti, R. K. R.; Thallapally, P. K.; Xue, F.; Mak, T. C. W.; Nangia, A. *Tetrahedron* 2**000**, *56*, 6707. (e) Broder, C. K.; Howard, J. A. K.; Keen, D. A.; Wilson, C. C.; Allen, F. H.; Jetti, R. K. R.; Nangia, A.; Desiraju, G. R. *Acta Crystallogr.* **2000**, *B56*, 1080. (f) Bosch, E.; Barnes, C. L. *Cryst. Growth Des.* **2002**, 299. (g) Eriksson, L.; Hu, J. *Acta Cryst.* **2002**, *E58*, 794. (h) Eriksson, L.; Hu, J. *Acta Crystallogr.* **2002**, *E58*, 1147.
(7) Csöregh, I.; Brehmer, T.; Bombicz, P.; Weber, E. *Cryst. Eng.* **2001**, *4*, 343.
(8) (a) Rahman, A. N. M. M.; Bishop, R.; Craig, D. C.; Scudder, M. L. *Cryst. Eng. Comm.* **2002**, *4*, 510. (b) Marjo, C. E.; Rahman, A. N. M. M.; Bishop, R.; Scudder, M. L.; Craig, D. C. *Tetrahedron* **2001**, *57*, 6289. (c) Tanaka, K.; Fujimoto, D.; Altreuther, A.; Oeser, T.; Irngartinger, H.; Toda, R. *J. Chem. Soc., Perkin Trans. 2* **2000**, 2115.
(9) (a) Creighton, J. A.; Thomas, K. M. *J. Chem. Soc., Dalton Trans.* **1972**, *403*. (b) Farina, A.; Meille, S. V.; Messina, M. T.; Metrangolo, P.; Resnati, G.; Veccia, G. *Angew. Chem., Int. Ed., Engl.* **1999**, *38*, 2433. (c) Freytag, M.; Jones, P. G.; Ahrens, B.; Fisher, A. K. *New J. Chem.* **1999**, 1137.
(10) (a) Yamamoto, H. M.; Yamaura, J.-I.; Kato, R. *J. Am. Chem. Soc.* **1998**, *120*, 5905. (b) Domercq, B.; Devic, T.; Fourmigue, M.; Auban-Senzier, P.; Canadell, E. *J. Mater. Chem.* **2001**, *11*, 1570.
(11) (a) Lu, J. Y.; Babb, A. M. *Inorg. Chem.* **2002**, *41*, 1339. (b) Morse, D. B.; Rauchfuss, T. B.; Wilson, S. R. *J. Am. Chem. Soc.* **1990**, *112*, 1860. (c) Ghassemazadeh, M.; Harms, K.; Dehnicke, K. *Chem. Ber.* **1996**, *129*, 259. (d) Grebe, J.; Geiseler, G.; Harms, K.; Dehnicke, K. *Zeit. Naturforsh. B: Chem. Sci.* **1999**, *54*, 77.
(12) (a) Willett R. D. *Mol. Cryst. Liq. Cryst., Sect. A* **1995**, *233*, 227. (b) Turnbull, M. M.; Albrecht, A. S.; Jameson, G. B.; Landee, C. P. *Mol. Cryst. Liq. Cryst.* **1999**, *335*, 245. (c) Matsumoto, T.; Miyazaki, Y.; Albrecht, A. S.; Landee, C. P.; Turnbull, M. M.; Sorai, M. *J. Phys. Chem. B.* **2000**, *104*, 9993. (d) Blanchette, J. T.; Willett, R. D. *Inorg. Chem.* **1988**, *27*, 843. (e) Rubenacker, G. V.; Waplak, S.; Hutton, S. L.; Haines, D. N.; Drumheller, J. E. *J. Appl. Phys.* **1985**, *57*, 3341. (f) Snivley, L. O.; Seifert, P. L.; Emerson, K.; Drumheller, J. E. *Phys. Rev. B* 1**979**, *20*, 2101. (g) Snivley, L. O.; Tuthill, G.; Drumheller, J. E. *Phys. Rev. B* **1981**, *24*, 5349−5355.
(13) (a) Patyal, B. R.; Scott, B. L.; Willett, R. D. *Phys. Rev.* **1990**, *B41*, 1657. (b) Landee, C. P.; Turnbull, M. M.; Galeriu, C.; Giantsidis, J.; Woodward, F. M. *Phys. Rev. B, Rapid Commun.* **2001**, *63*, 100402R.
(14) Tulsky, E. G.; Long, J. R. *Chem. Mater.* **2001**, *13*, 1149.
(15) (a) Halvorson, K. E.; Grigereit, T.; Willett, R. D. *Inorg. Chem.* **1987**, *26*, 1716. (b) Geiser, U.; Willett, R. D.; Lindbeck, M.; Emerson, K. *Inorg. Chem.* **1986**, *25*, 1173. (c) Willett, R D.; Geiser, U. *Acta Chem. Croat.* **1984**, *57*, 751. (d) Bond, M. R.; Willett, R. D. *Inorg. Chem.* **1984**, *28*, 3267. (e) Willett, R. D.; Bond, M. R.; Pon, G. *Inorg. Chem.* **1990**, *29*, 4160. (f) Willett, R. D. *Acta Crystallogr.* **1993**, *A49*, 613. (g) Weiss, S.; Willett, R. D. *Acta Crystallogr.* **1993**, *B49*, 283. (h) Willett, R. D.; Place, H.; Middleton, M. *J. Am. Chem. Soc.* **1988**, *110*, 8639.
(16) Freytag, M.; Jones, P. G.; Ahrens, B.; Fischer, A. K. *New J. Chem.* **1999**, *23*, 1137.
(17) (a) Luque, A.; Sertucha, J.; Casillo, O.; Romain, P. *New J. Chem.* **2001**, *25*, 1208. (b) Luque, A.; Sertucha, J.; Casillo, O.; Romain, P. *Polyhedron* **2002**, *21*, 19.
(18) (a) Haddad, S.; Willett, R. D. *Inorg. Chem.* **2001**, *40*, 2457. (b) Haddad, S.; Willett, R. D. *J. Chem. Cryst.* **2001**, *31*, 37.
(19) Coffey, T. J.; Landee, C. P.; Robinson, W. T.; Turnbull, M. M.; Winn, M.; Woodward, F. M. *Inorg. Chim. Acta* **2000**, *303*, 54.
(20) Place, H.; Willett, R. D. *Acta Crystallogr.* **1987**, *C43*, 1497.
(21) Place, H.; Willett, R. D., unpublished results.

(22) Haddad, S.; Willett, R. D. *Acta Cryst.* **2000**, *C56*, e437.
(23) Place, H.; Willett, R. D. *Acta Crystallogr.* **1987**, *C43*, 1050.
(24) Woodward, F. M.; Landee, C. P.; Giantsidis, J.; Turnbull, M. M.; Richardson, C. *Inorg. Chim. Acta* **2001** *324*, 324.
(25) Landee, C. P.; Turnbull, M. M., private communication.
(26) Twamley, B.; Willett, R. D., unpublished results.
(27) Luque, A.; Sertucha, J.; Lezama, L.; Rojo, T.; Romain, P. *J. Chem. Soc., Dalton Trans.* **1997**, 847.
(28) Campana, C. F.; Shepherd, D. F.; Litchman, W. M. *Inorg. Chem.* **1981**, *20*, 4039.
(29) Sheldrick, G. SHELXTL, Nicolet Analytical Corporation, Madison, WI, USA, 1984.
(30) XSCANS, Siemen Analytical X-ray Instrument, Inc., Version 2.00, Madison, WI, USA, 1993.
(31) SHELXTL (XCIF, XL, XP, XPREP, XS), Version 6.10, Bruker AXS Inc., Madison, WI, USA, 2002.
(32) SMART, Version 5.625, Bruker AXS Inc., Madison, WI, USA, 2002.
(33) SAINTPlus V 6.22, Bruker AXS, Inc., Madison, WI, USA, 2001.
(34) SADABS V 2.03, Bruker AXS Inc., Madison, WI, USA, 2001.

CG030003Y